Chapter 13

NOISE

An important and fundamental limitation in the performance of all electron tubes and their associated circuits is noise. In this chapter we shall consider noise to be unwanted signals having a random or incoherent nature. The effects of noise may be of greater or lesser importance in communications systems, depending on the type of modulation used and the level of the intelligence-bearing signal relative to that of the noise. Noise may obscure weak signals in the case of amplitude or frequency modulation systems, and it may give false signals in pulse code modulation systems.

The word "noise" is also often used to include unwanted man-made signals, such as those due to electric motors, diathermy machines, automobile ignitions, transmitter harmonics, etc. However, such signals can be reduced to tolerable levels at their sources by proper engineering, and we shall not further consider this type of noise.

Random noise results from the finite charge on the electron or other carriers within the conductors and devices used in electronic circuits. Because an electric current within a conductor or an electron beam is made up of individual charged particles in motion, and because each particle carries a finite discrete charge, the current flow is never continuous but is subject to statistical fluctuations about an average value.

We shall find that the induced current flowing in the external circuit of a temperature-limited diode is characterized by a mean-square fluctuation current, or noise current, given by

$$\overline{i^2} = 2eI_{So}\Delta f \tag{13-1}$$

where $-e$ is the electronic charge, I_{So} is the dc beam current, and Δf is the bandwidth over which the noise current is measured. This expression is valid only when the electron transit time is small compared with the period of the noise frequencies under observation. Noise resulting from a current flow which is limited by the random passage of electrons over a potential

barrier, such as the potential barrier at the surface of a temperature-limited cathode, is known as shot noise.

A second fundamental source of random noise results from the thermal motions of electrons or other charge carriers within a resistance. The motion of the charge carriers within the resistance causes a noise voltage to appear across the terminals of the resistance. We shall find that the mean square noise voltage across a resistance R is given by

$$\overline{v^2} = 4kTR\Delta f \tag{13-2}$$

where k is Boltzmann's constant, equal to 1.38×10^{-23} joules/°K, T is the absolute temperature of the resistance, and Δf is the bandwidth over which the noise voltage is measured. If the resistance is connected to a second resistance, noise power is transmitted from the first resistance to the second resistance, and likewise noise power is transmitted from the second resistance to the first resistance. Maximum noise power is transmitted from one resistance to the other when the two resistances are equal. This maximum transmitted noise power, or the available noise power from the resistance, is given by

$$P = kT\Delta f \tag{13-3}$$

In grid-controlled tubes, the individual electrons of the beam pass the control grid at random times with the result that noise currents are induced in the grid circuit. This leads to a noise voltage at the control grid, and this noise voltage is amplified by the tube. Still another kind of noise, called partition noise, appears in the output of grid-controlled tubes and beam-type tubes when an electrode such as a screen grid intercepts a portion of the electron beam and hence adds random fluctuations to the remainder of the beam current. This type of noise is closely related to shot noise.

In beam-type microwave tubes, the random nature of the electron emission time and emission velocity gives rise to initial current and velocity modulation on the electron beam, and this in turn is amplified.

Noise sets a limit to the smallest signal that an amplifier can detect. The noise at the output of an amplifier consists of the amplified thermal noise due to the resistance of the source plus the noise added by the amplifier itself. For high receiver sensitivity, the noise added by the amplifier should be as small as possible.

The noise performance of an amplifier is specified by a quantity termed the noise figure (or noise factor). The noise figure F is defined by[1]

$$F = \frac{\mathcal{G}_a kT_o B + N_a}{\mathcal{G}_a kT_o B} = 1 + \frac{N_a}{\mathcal{G}_a kT_o B} \tag{13-4}$$

[1]References 13.1, 13.2. Available power is the power delivered to a matched load. Available power gain is the ratio of available powers at the output and input of an amplifier.

where N_a is the total available noise power due to noise sources within the amplifier, $\mathcal{G}_o$ is the available power gain of the amplifier at band center, T_o is a standard reference temperature equal to 290°K, and B is the amplifier bandwidth. The bandwidth B is defined as

$$B = \frac{1}{\mathcal{G}_o} \int_0^\infty \mathcal{G}(f) df \tag{13-5}$$

where $\mathcal{G}(f)$ is the available power gain at frequency f. The quantity $\mathcal{G}_o k T_o B$ in Equation (13-4) is then the total available noise power output for an ideal noiseless amplifier with the same variation of available power gain with frequency. Equation (13-4) states that the noise figure is equal to the ratio of the total available output noise to the available noise which would be present at the output if the amplifier itself were noiseless, assuming a source temperature of 290°K. The noise figure is usually expressed in decibels; that is, ten times the logarithm to the base 10 of the above quantity.

The expression for noise figure may be written in another form. The available signal power at the input S_{in} is related to the available signal power at the output S_{out} by

$$S_{out} = \mathcal{G}_o S_{in} \tag{13-6}$$

Equation (13-4) may thus be written

$$F = \frac{\dfrac{S_{in}}{kT_oB}}{\dfrac{S_{out}}{\mathcal{G}_o kT_oB + N_a}} = \frac{\dfrac{S_{in}}{N_{in}}}{\dfrac{S_{out}}{N_{out}}} \tag{13-7}$$

where N_{in} and N_{out} are the available noise powers at the input and output, respectively, assuming the standard source temperature.

The noise figure defined above is sometimes called the average noise figure, since the noise power is averaged over the entire bandwidth of the amplifier. Alternatively, for wide-band amplifiers, it is sometimes desirable to know the *spot noise figure*, a function of frequency. The spot noise figure is defined as above, except that noise power is measured in some small unit frequency interval centered at the signal frequency. B in the above equations is then replaced by this unit frequency interval.

The above definitions of noise figure assume a standard source temperature T_o of 290°K, room temperature. This is convenient for noise figure measurements. However, receivers are sometimes operated with receiving antennas pointed toward the sky. Under such conditions, the effective source temperature is often considerably less than room temperature.[2] At

[2]Reference 13.3.

frequencies proposed for satellite communications, 1 to 10 Gc, the effective sky temperature may be as low as 4°K. Let us examine the applicability of the noise figure concept under these conditions.

The available output noise added by the amplifier is obtained from Equation (13-4) as

$$N_a = (F - 1)kT_oB\mathcal{G}_o \tag{13-8}$$

The total available output noise for a source at temperature T_s is given by

$$\begin{aligned} N_{\text{out}}' &= kT_sB\mathcal{G}_o + N_a \\ &= kT_sB\mathcal{G}_o\left[1 + \frac{T_o}{T_s}(F - 1)\right] \end{aligned} \tag{13-9}$$

where the prime indicates that the actual source temperature is indicated. Using Equation (13-6), this may be written as

$$\frac{S_{\text{in}}}{kT_sB} = \frac{S_{\text{out}}}{N_{\text{out}}'}\left[1 + \frac{T_o}{T_s}(F - 1)\right] \tag{13-10}$$

which relates the signal-to-noise ratios at the input and output of the amplifier.[3]

Equation (13-10) may be used to determine the minimum detectable input signal for a receiver. Suppose that we ask: How weak can the input signal be and still be distinguished from the noise? The signal-to-noise ratio at the output corresponding to this condition is somewhat arbitrary, so we shall take it as unity. That is, we shall set $S_{\text{out}}/N_{\text{out}}' = 1$. This corresponds to a doubling of the output power as a criterion to determine the presence of a signal.

The minimum detectable input signal S_{in} from Equation (13-10) is plotted in Figure 13-1 as a function of noise figure for $S_{\text{out}}/N_{\text{out}}' = 1$ and for three source temperatures. The receiver bandwidth is taken arbitrarily as 1 Mc. Values for other bandwidths are easily obtained, since the minimum detectable input signal is directly proportional to the receiver bandwidth. For a source at room temperature, the relationship between minimum detectable input signal and noise figure is linear. However, for lower source temperatures, the minimum detectable input signal decreases more rapidly with decreasing noise figure. Thus, considerable improvement is realized by using low noise figure receivers ($F < 5$ db) in systems whose receiving antennas are directed toward the sky.

---

[3]Another useful noise quantity is the *effective input noise temperature* of the amplifier, equal to $T_o(F - 1)$. This is the temperature of an equivalent noise source at the input of an equivalent noiseless amplifier which replaces the actual amplifier. It is useful because it gives the relative contribution of the amplifier to the total output noise for any source temperature.

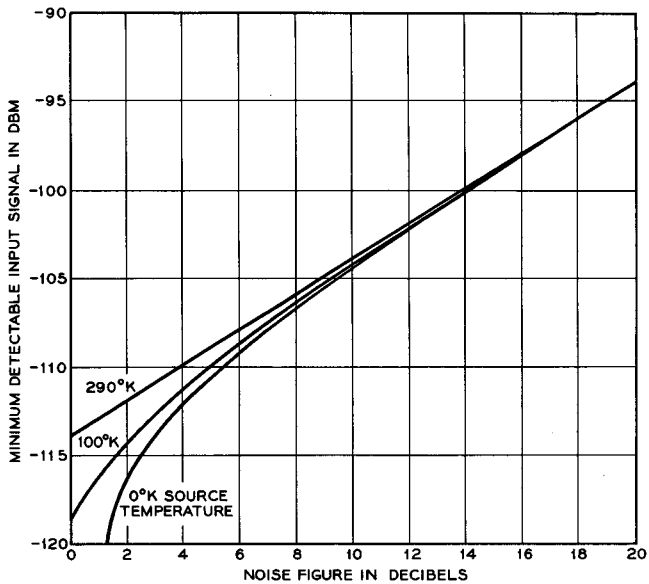

FIG. 13-1 Receiver sensitivity for a bandwidth of 1 Mc for signal sources at various temperatures as a function of the receiver noise figure. The signal-to-noise ratio at the receiver output is assumed to be unity.

We shall use the noise figure concept at several places in this chapter as a measure of the noise performance of an amplifier.

13.1 Fundamental Sources of Noise

There are certain fundamental sources of noise due to the fact that electron current is composed of individual electrons, each with its own velocity and position. Statistical methods have been used to analyze these effects.[4] Most of the analyses are rather complex for an introductory study of noise; hence, we shall limit our discussion to nonrigorous demonstrations of the fundamental theorems.

(a) *Thermal Noise*

Any passive resistance acts as a noise source with an available noise power given by Equation (13-3). The available noise power is the power

[4]Reference 13.4.

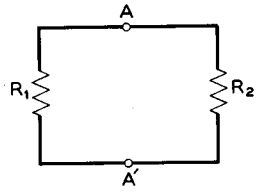

FIG. 13.1-1 Two equal resistors at different temperatures connected together. R_1 is at temperature T_1, and R_2 is at temperature T_2.

which is delivered to a matched load. Thus in Figure 13.1-1, if $R_1 = R_2$, a power $kT_1\Delta f$ flows from R_1 to R_2 within the frequency range Δf, and similarly $kT_2\Delta f$ flows from R_2 to R_1 within the frequency range Δf, where T_1 and T_2 are the respective resistor absolute temperatures. If $T_1 > T_2$, energy is transferred from R_1 to R_2. If the resistors are at the same temperature, no net transfer of energy occurs; the powers flowing in the two directions are equal.

Equivalent circuits for a resistor as a noise source are given in Figure 13.1-2. $\overline{v^2}$ and $\overline{i^2}$ indicate time averages of the square of the voltage and current, respectively. An equivalent rms quantity would be given by the

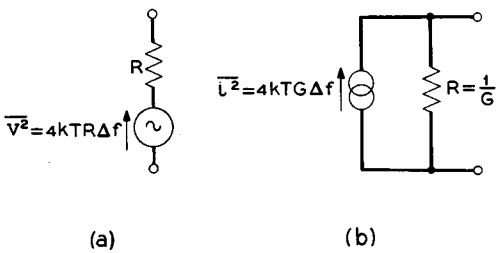

FIG. 13.1-2 Equivalent circuits for the thermal noise associated with a passive resistance. R in these equivalent circuits is taken to be noiseless. (a) Voltage source equivalent circuit. (b) Current source equivalent circuit.

square root of such a quantity. It is simple to demonstrate that each of these circuits has an available power equal to $kT\Delta f$. The resistor in each equivalent circuit is considered noiseless; the voltage and current sources represent the only sources of noise.

As an example of the use of these equivalent circuits, let us determine the exchange of energy for the circuit of Figure 13.1-1, where $R_1 \neq R_2$ and $T_1 \neq T_2$. The equivalent circuit is shown in Figure 13.1-3, using the voltage source equivalent circuit of Figure 13.1-2(a). The two noise sources are uncorrelated. That is, the random electron motion of one resistor is completely independent of that of the other resistor. Thus, if we were to compare the relative phases of the two sources in a very narrow bandwidth, the phase difference could be anywhere from zero to 360 degrees, with equal probability, and is continuously varying. Each source acts completely independently of the other. We may use a very special type of superposition

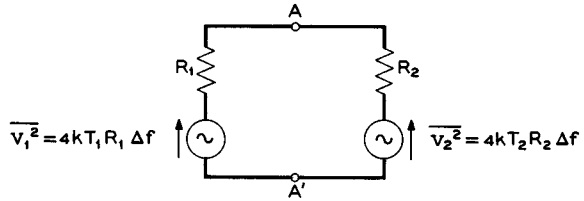

FIG. 13.1-3 Noise equivalent circuit for two unequal resistors R_1 and R_2, having temperatures T_1 and T_2, respectively, connected together.

in these problems of uncorrelated noise sources: The noise power delivered from each source to the other parts of the circuit may be evaluated by computing power with all other sources set to zero. Thus, in Figure 13.1-3 the power delivered to R_2 from R_1 is given by

$$P_{12} = \frac{\overline{v_1^2}R_2}{(R_1 + R_2)^2} = \frac{4kT_1R_1R_2\Delta f}{(R_1 + R_2)^2} \tag{13.1-1}$$

Similarly, the power delivered to R_1 from R_2 is

$$P_{21} = \frac{\overline{v_2^2}R_1}{(R_1 + R_2)^2} = \frac{4kT_2R_1R_2\Delta f}{(R_1 + R_2)^2} \tag{13-1.2}$$

The net flow of power from R_1 to R_2 is

$$P_{12} - P_{21} = \frac{4k(T_1 - T_2)R_1R_2\Delta f}{(R_1 + R_2)^2} \tag{13.1-3}$$

If $R_1 = R_2 = R$, we have

$$P_{12} - P_{21} = k(T_1 - T_2)\Delta f \tag{13.1-4}$$

which agrees with our previous result.

As another example, we shall determine the noise voltage appearing across the terminals A-A' in Figure 13.1-1. This voltage would be of interest in the case where the resistors shown comprise the grid circuit in an

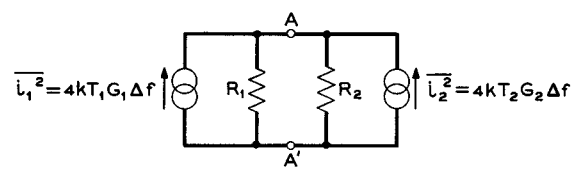

FIG. 13.1-4 Noise equivalent circuit of two resistors in parallel, both at the same temperature. It is demonstrated that the noise properties are given by the thermal noise of the equivalent parallel resistor.

amplifier; this noise voltage multiplied by the voltage gain of the amplifier appears as a portion of the output noise of the amplifier.

The noise voltage appearing across terminals A-A' is most readily determined using the current source equivalent circuit of Figure 13.1-2(b). The noise equivalent circuit for the two resistors is shown in Figure 13.1-4. For convenience, we define the conductances $G_1 = 1/R_1$, $G_2 = 1/R_2$, and $G_T = G_1 + G_2 = 1/R_T$. The total noise voltage is obtained by superposition of the mean-square voltages produced by each noise source. The total noise voltage is given by

$$\overline{v_T^2} = \frac{4kT_1G_1\Delta f}{G_T^2} + \frac{4kT_2G_2\Delta f}{G_T^2}$$

$$= 4k\Delta f\frac{T_1G_1 + T_2G_2}{G_T^2} \tag{13.1-5}$$

If $T_1 = T_2 = T$, Equation (13.1-5) becomes

$$\overline{v_T^2} = 4kTR_T\Delta f \tag{13.1-6}$$

which is the open-circuit voltage of Figure 13.1-2(a), with R replaced by R_T, the equivalent resistance of the parallel combination of resistors. This is a special case of a more general theorem; that is, the available output noise power at any two terminals of a passive isothermal network is equal to $kT\Delta f$.[5] Thus, the noise at two terminals of any passive isothermal network may be obtained from the equivalent circuits of Figure 13.1-2, where R in Figure 13.1-2(a) is given by the real part of the two-terminal impedance and $1/R$ in Figure 13.1-2(b) is given by the real part of the two-terminal admittance.

Noise calculations in circuits containing reactive elements are made using the equivalent circuits of Figure 13.1-2 and the rules of ac circuit analysis. As an example let us compute the noise current flowing in an R-L-C loop. The impedance of the loop is given by

$$|Z| = \sqrt{R^2 + (\omega L - 1/\omega C)^2}$$

Using the equivalent circuit of Figure 13.1-2(a), the noise current is given by

$$\overline{i^2} = \frac{\overline{v^2}}{|Z|^2} = \frac{4kTR\Delta f}{R^2 + (\omega L - 1/\omega C)^2}$$

A simple derivation of the expression for thermal noise, Equation (13-3), proceeds as follows.[6] In Figure 13.1-5 are shown two identical resistors of

[5]This general theorem requires only that each resistor possess bilateral network properties with respect to the output terminals. See Reference 13.4, pp. 185–189.

[6]Reference 13.5.

resistance R joined by a lossless TEM transmission line of characteristic impedance R. All parts of the circuit are at a temperature T. Since the transmission line is matched at both ends, each resistor is delivering its available power to the line. This power then flows to the other resistor where it is dissipated.

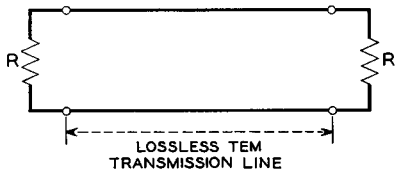

FIG. 13.1-5 A transmission line terminated in its characteristic impedance R at both ends. The line and the terminating resistors are all at the same temperature T.

Now, suppose that the line is suddenly shorted at both ends. The shorted line is a resonant element with resonant frequencies corresponding to the line length L being an integral number of half wavelengths, that is

$$f_n = \frac{nc}{2L} \tag{13.1-7}$$

where c is the velocity of propagation on the line, and n is an integer. Thus the modes of oscillation are spaced by a frequency interval Δf, where

$$\Delta f = \frac{c}{2L} \tag{13.1-8}$$

From the equipartition theorem of statistical mechanics,[7] each mode of oscillation will have associated with it an energy kT. Now the standing wave corresponding to the resonant mode is comprised of two traveling waves, traveling in opposite directions. Hence, each traveling wave has an energy $\frac{1}{2}\,kT$ and an energy per unit length given by

$$W_l = \frac{kT}{2L} \tag{13.1-9}$$

Since the group velocity for a TEM transmission line is c, the power flow in one direction P is given by

$$P = cW_l = \frac{kTc}{2L} \tag{13.1-10}$$

We may substitute for L from Equation (13.1-8) obtaining

$$P = kT\Delta f \tag{13.1-11}$$

Since the line was shorted instantaneously, this must also be the power flow in each direction before the lines were shorted. Thus, each resistor has an available noise power given by Equation (13.1-11). A rigorous development of an expression for thermal noise is outlined in Appendix XVI.

[7]Reference 13a, Chapter 11.

(*b*) *Shot Noise*

In an electron tube the cathode emission current consists of individual electrons emitted at random. The random emission times for the individual electrons result in fluctuations of the current induced in the output circuit. The noise associated with these fluctuations is known as shot noise.

When the current drawn from the cathode is space charge limited, the space charge near the cathode acts to reduce the shot noise, an effect which will be studied later. On the other hand, when the emission is temperature limited, full shot noise is obtained. Diodes operated with temperature-limited emission are often used as standard noise sources.

The magnitude of full shot noise for a diode can be evaluated by statistical methods. Full shot noise is given by a current source of mean-square value[8]

$$\overline{i^2} = \frac{8eI_{So}}{(\omega\tau)^4}[(\omega\tau)^2 + 2(1 - \cos\omega\tau - \omega\tau\sin\omega\tau)]\Delta f \qquad (13.1\text{-}12)$$

for a planar diode, where I_{So} is the temperature limited dc current, and τ is the electron transit time. The ac current i is equal to the difference between the instantaneous value of the current and the average value, and $\overline{i^2}$ indicates the time average of the square of this quantity. Equation

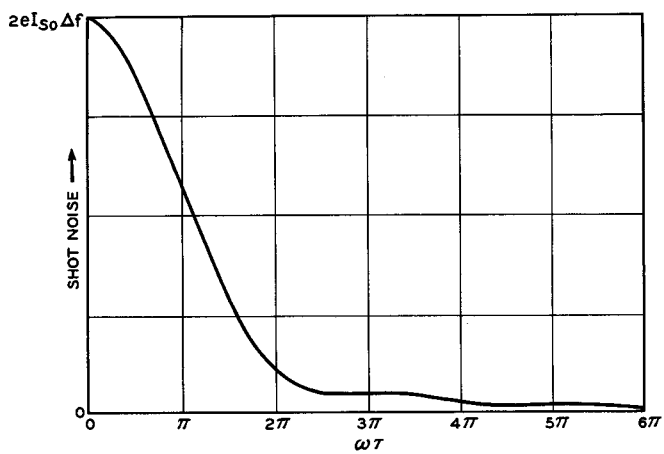

FIG. 13.1-6 Variation of full shot noise with transit angle in a parallel-plane diode (From *An Introduction to the Theory of Random Signals and Noise*, by W. B. Davenport and W. L. Root. Copyright 1958. McGraw-Hill Book Co., Inc. Used by permission)

[8]Reference 13.4, Chapter 7.

(13.1-12) is plotted in Figure 13.1-6. At low frequencies, full shot noise is given by

$$\overline{i^2} = 2eI_{So}\Delta f \tag{13.1-13}$$

The latter expression holds for diodes of any geometry. It is to be noted that full shot noise is not a function of temperature; one might expect this since it is caused by random emission time.

A simple derivation of Equation (13.1-13) proceeds as follows.[9] Consider the vacuum tube shown in Figure 13.1-7 consisting of two identical, planar, close-spaced cathodes parallel to each other. The entire structure is assumed to be enclosed in an isothermal oven at temperature T. Each cathode emits a small temperature limited current with noise fluctuations, intercepted by the opposite cathode, so that a noise current flows in the external wire connecting the two cathodes. This noise current is equal to

$$\overline{i^2} = 4kTG\Delta f \tag{13.1-14}$$

from Figure 13.1-2, where G is the ac conductance of the diode formed by the two cathodes. This formula applies to the diode since it is a passive, isothermal structure in thermal equilibrium.

Next we must evaluate the ac conductance of the diode. This conductance is equal to $\partial I_o/\partial V_o$ in the limit as both the diode current I_o and

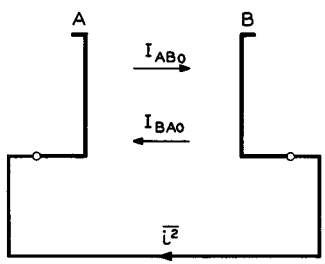

FIG. 13.1-7 Isothermal structure consisting of two identical, planar, close-spaced cathodes parallel to each other.

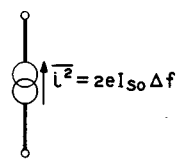

FIG. 13.1-8 Equivalent circuit for the noise from a temperature-limited diode at low frequencies.

the diode voltage V_o approach zero. In order to evaluate the functional relationship between I_o and V_o let us assume that cathode A is positive with respect to cathode B, the potential difference being equal to V_o. The diode current I_o is given by

$$I_o = I_{ABo} - I_{BAo} \tag{13.1-15}$$

[9]Reference 13.6.

where I_{ABo} corresponds to the current of electrons emitted from cathode B arriving at cathode A, and I_{BAo} corresponds to the current of electrons emitted from cathode A arriving at cathode B.

Since electrode A is positive, I_{ABo} is equal to the maximum or saturated value of temperature limited current, which we call I_{So}. On the other hand, the electrons emitted from cathode A see a repelling field so that only the electrons with normally directed emission energy greater than eV_o electron volts are able to escape from A and arrive at B. The probability distribution function for the emitted electrons is given by Equation (2.4-2) as a function of the kinetic energy associated with the normally directed velocity. The fraction of the emitted electrons with energies sufficient to overcome the potential barrier is obtained from this equation as:

$$\frac{I_{BAo}}{I_{So}} = \frac{\frac{1}{W_T}\int_{eV_o}^{\infty} \epsilon^{-W_n/W_T} dW_n}{\frac{1}{W_T}\int_{0}^{\infty} \epsilon^{-W_n/W_T} dW_n} = \epsilon^{-eV_o/kT} \tag{13.1-16}$$

Thus, the total current is given by

$$I_o = I_{So} - I_{So}\epsilon^{-eV_o/kT} \tag{13.1-17}$$

For V_o approaching zero, the conductance is given by

$$G = \left.\frac{\partial I_o}{\partial V_o}\right|_{V_o=0} = \frac{eI_{So}}{kT} \tag{13.1-18}$$

from Equation (13.1-17).

When the value of conductance given by the last equation is substituted into Equation (13.1-14), one obtains

$$\overline{i^2} = 4kTG\Delta f = 4eI_{So}\Delta f$$

This noise current is the sum of two equal uncorrelated shot noise currents — that due to cathode A and that due to cathode B. For a single cathode the shot noise is half of this, or

$$\overline{i^2} = 2eI_{So}\Delta f$$

identical with Equation (13.1-13).

The low-frequency equivalent circuit of the temperature limited diode for noise calculations is given in Figure 13.1-8.

(c) *Velocity Fluctuations*

In addition to a random emission time, each electron possesses a random emission velocity. In low-frequency tubes operating under space-charge limited conditions, we shall find in the next section that it is the randomness

of the electron velocity which sets a limit to the minimum noise. In microwave tubes, the velocity fluctuations act as initial velocity modulation on the electron beam, which may be amplified to produce output noise.

The probability distribution function for the normal component of electron emission velocity is given by Equation (1) of Appendix IV as

$$dP(u_n) = \frac{mu_n}{kT_c}\epsilon^{-mu_n^2/2kT_c}du_n \tag{13.1-19}$$

where T_c is the cathode temperature. As the emitted electrons move toward the potential minimum, those of lowest velocity are continuously sorted out and returned to the cathode.

Let us calculate the average velocity of the forward moving electrons at any point between the cathode and the potential minimum. The normal component of velocity of an electron at a point where the electrostatic potential relative to the cathode is V may be written in terms of the emission component u_n as

$$u^2 = u_n^2 + 2\frac{e}{m}V \tag{13.1-20}$$

Since the electrostatic potential is independent of an individual electron's velocity, Equation (13.1-20) leads to

$$udu = u_n du_n \tag{13.1-21}$$

Thus, Equation (13.1-19) can be written as

$$dP(u) = \frac{mu}{kT_c}\epsilon^{-(m/2kT_c)(u^2-2eV/m)}du \tag{13.1-22}$$

The average velocity of the electrons moving away from the cathode at a point between the cathode and the potential minimum where the potential relative to the cathode is V is given by

$$\bar{u} = \frac{\displaystyle\int_0^\infty \frac{mu^2}{kT_c}\epsilon^{-(m/2kT_c)(u^2-2eV/m)}du}{\displaystyle\int_0^\infty \frac{mu}{kT_c}\epsilon^{-(m/2kT_c)(u^2-2eV/m)}du}$$

$$= \sqrt{\frac{\pi kT_c}{2m}} \tag{13.1-23}$$

a constant. This is an interesting result. Since $\bar{u}$ is independent of V, we must conclude that even though all electrons are being slowed down by the repelling field of the potential minimum, the average velocity of those passing the potential minimum is constant. Moreover, this average velocity is also independent of the potential difference between the cathode and

the potential minimum. Thus, $\bar{u}$ remains constant even though the potential mimimum fluctuates due to some noise perturbation.

The average velocity given by Equation (13.1-23) is an average taken over a sufficiently long length of time. At any particular time the average electron velocity may be slightly higher or slightly lower than this value. The mean-square fluctuation of the average velocity at the potential minimum can be shown to be[10]

$$\overline{u_A^2} = \frac{ekT_c\Delta f}{m\bar{I}_{ao}}(4 - \pi) \tag{13.1-24}$$

where I_{ao} is the dc anode current. u_A is the difference between the instantaneous value of the average velocity at the potential minimum and the value given by Equation (13.1-23), and $\overline{u_A^2}$ is the time average of the square of this quantity.

(*d*) *Space-Charge Smoothing*

When tubes are operated under space-charge limited conditions, the output noise is found to be considerably less than that corresponding to full shot noise. Thus, if the noise is represented by a current source in the plate circuit, it is of a strength,

$$\overline{i^2} = \Gamma^2 \cdot 2eI_{ao}\Delta f \tag{13.1-25}$$

where transit-time effects are assumed to be negligible, I_{ao} is the dc anode current, and Γ^2 is a factor less than unity.

A physical explanation of the space-charge smoothing of the shot noise is easily given. Potential profiles for a space-charge limited diode are shown in Figure 13.1-9. The equilibrium potential profile is shown as a solid line. If, due to shot noise fluctuations, a larger than average number of electrons is emitted at a particular instant, the potential minimum would be depressed slightly as indicated by curve A. Because of the deepening of this minimum, a smaller percentage of the emitted electrons is able to pass the minimum and go on to the anode. Only those electrons with sufficiently high emission velocities can pass the minimum. Thus, the higher instantaneous emission current is somewhat neutralized by the rejection of a larger percentage of the emitted electrons by the deeper potential minimum. Curve B corresponds to the opposite situation, where a fewer-than-average number of electrons are emitted at a particular instant. In this case, there is less space charge in front of the cathode, the potential minimum becomes shallower, and a larger percentage of the emitted electrons pass on to the anode.

---

[10]Reference 13.7.

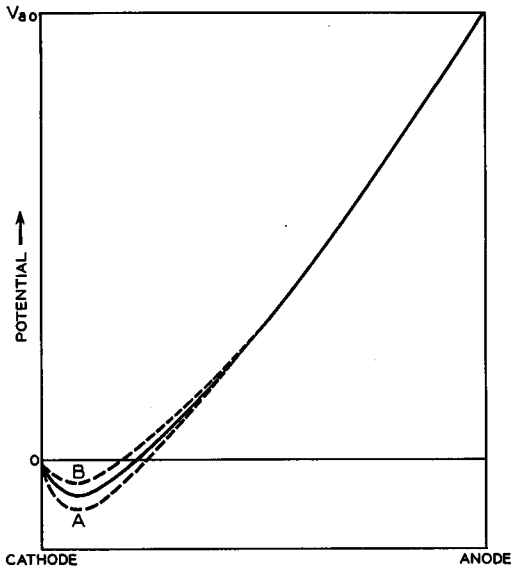

FIG. 13.1-9 Potential distribution in a space-charge limited diode under equilibrium conditions (heavy line). Dotted curves A and B indicate the potential distributions obtained due to an instantaneous excess or deficiency of emitted current, respectively.

This space-charge smoothing process is indeed very effective. At low frequencies, the current fluctuations are reduced greatly. Γ^2 may be as low as 0.02.

We can derive a simple expression for the space-charge smoothing factor Γ^2 using the Llewellyn and Peterson equations of Section 7.2.[11] The Llewellyn and Peterson equations are given by Equations (7.2-1), and the coefficients are tabulated in Appendix XI. The equations are applied to an open-circuited diode; that is, the diode is operated with an rf open circuit such as is obtained with a series rf choke of high inductance. We shall derive the noise-fluctuation voltage appearing across the diode.

In Figure 7.2-1(a) we take the potential minimum to correspond to plane A and the anode to correspond to plane B. The first of Equations (7.2-1) (symbols as defined in Section 7.2) may be written as

$$V_B - V_A = B^* J_A + C^* U_A \tag{13.1-26}$$

since $J_T = 0$ for an open-circuited diode. From Appendix XI we have

$$\zeta = 1 \tag{13.1-27}$$

[11]Reference 13.7.

for a space-charge limited diode, and

$$u_{Ao} = 0 \tag{13.1-28}$$

corresponding to zero dc velocity at the potential minimum, so that

$$B^* = \frac{T^2}{\varepsilon_o \beta^3} u_{Ao}[2P - \beta Q] = 0 \tag{13.1-29}$$

and

$$C^* = -\frac{2m}{e} u_{Bo} \frac{P}{\beta^2} \tag{13.1-30}$$

At low frequencies, β approaches zero and

$$\frac{P}{\beta^2} \to \frac{1}{2} \tag{13.1-31}$$

so that C^* is given by

$$C^* = -\frac{m}{e} u_{Bo} \tag{13.1-32}$$

Thus, from Equations (13.1-26), (13.1-29), and (13.1-32), we have

$$\overline{v^2} = \left(\frac{m}{e} u_{Bo}\right)^2 \overline{u_A^2} = \frac{2m}{e} V_{ao} \overline{u_A^2} \tag{13.1-33}$$

where $\overline{v^2}$ is the mean-square voltage fluctuation across the open-circuited diode, and $\overline{u_A^2}$ is the mean-square velocity fluctuation at the potential minimum; V_{ao} is the dc anode voltage. But, as discussed in part (c) above, $\overline{u_A^2}$ is given by Equation (13.1-24). Thus, Equation (13.1-33) may be written as

$$\overline{v^2} = 2kT_c \Delta f \frac{V_{ao}}{I_{ao}} (4 - \pi) \tag{13.1-34}$$

Equation (13.1-34) may be written in a more useful form. Let us define the dynamic resistance of the diode as

$$r_a = \frac{dV_{ao}}{dI_{ao}} \tag{13.1-35}$$

as in Appendix X. Since the space-charge limited diode current is proportional to the three-halves power of the voltage, we have

$$r_a = \frac{2}{3} \frac{V_{ao}}{I_{ao}} \tag{13.1-36}$$

Thus, Equation (13.1-34) may be written as

$$\overline{v^2} = 4k\theta T_c r_a \Delta f \tag{13.1-37}$$

where $\theta = 3(1 - \pi/4) = 0.644$. Comparing this with the corresponding expression for thermal noise, we see that the diode appears as a thermal noise source whose temperature is 0.644 times the cathode temperature. The equivalent circuit is given in Figure 13.1-10.

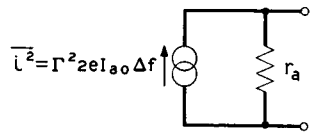

FIG. 13.1-10 Equivalent circuit for the noise from a space-charge limited diode. The resistance r_a is noiseless.

The reader may wonder why the formula for thermal noise does not apply directly, that is, why θ should not be unity. The reason for this is that the space-charge limited diode is not in thermal equilibrium, a necessary condition for the validity of the thermal noise available power expression. By virtue of the dc current, chemical energy from an external dc voltage source is being converted into the heat associated with plate dissipation. On the other hand, the tube of Figure 13.1-7 corresponded to thermal equilibrium since no dc voltages were applied to it; thus thermal noise formulas could be applied directly.

Converting Equation (13.1-37) to an equivalent current source and comparing with Equation (13.1-25), we obtain an expression for Γ^2,

$$\Gamma^2 = \frac{3k\theta T_c}{eV_{ao}} \tag{13.1-38}$$

For a typical oxide-coated cathode, with $T_c = 1000°K$, this becomes

$$\Gamma^2 = \frac{0.167}{V_{ao}} \tag{13.1-39}$$

with V_{ao} in volts.

Practical diodes usually produce more noise than is predicted by the above expressions. In high-current diodes, the noise may be an order of magnitude greater. This is due in part to elastic reflections of electrons at the anode. The reflected electrons find their way back to the potential minimum where they increase the fluctuations in the current passing the potential minimum. Triodes, on the other hand, show good agreement with the above expressions, since the negative grid deflects the reflected electrons and prevents most of them from returning to the potential minimum.[12]

The results of this section are applicable only to low frequencies, where transit times are negligible. Effects at higher frequencies will be considered later.

---

[12]Reference 13.8.

13.2 Noise in Grid-Controlled Tubes

Triodes, tetrodes, and pentodes have other sources of noise in addition to shot noise. In this section we shall study these other noise sources, and in addition we shall consider the modification of the shot noise expression so that it will apply to grid-controlled tubes.

The equivalent circuit for the noise sources of a tetrode or pentode is shown in Figure 13.2-1.[13] The reduced shot noise is given by $\overline{i_s^2}$. In tetrodes and pentodes there is partition noise $\overline{i_p^2}$ due to the random interception of current by the screen grid. The screen-grid noise current $\overline{i_{sg}^2}$ is

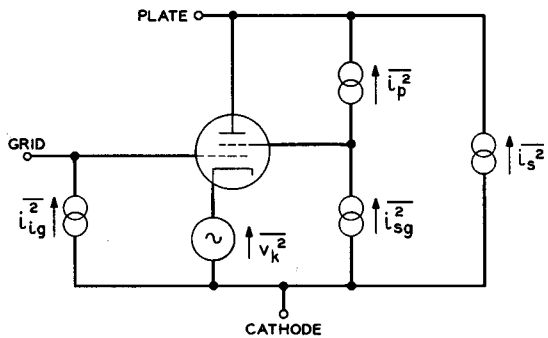

FIG. 13.2-1 Equivalent circuit for the noise of a tetrode or pentode. The noise sources are as follows:

i_{ig}^2 Induced grid noise
i_p^2 Partition noise
i_s^2 Shot noise
i_{sg}^2 Screen grid interception noise
v_k^2 Cathode-coating noise

usually eliminated as a noise contributor by means of a bypass capacitor from screen grid to the cathode. The induced grid noise is represented by the generator $\overline{i_{ig}^2}$; this noise results from fluctuations of induced grid current due to the electrons in the cathode-grid region. Finally, cathode-coating noise or flicker noise is represented by the voltage source $\overline{v_k^2}$. All of these noise sources will be discussed in detail in this section.

The same equivalent circuit applies to a triode, except that the sources $\overline{i_p^2}$ and $\overline{i_{sg}^2}$ are eliminated.

Certain simplifications of the equivalent circuit are possible at high and low frequencies. Above 100 kc the flicker noise is usually negligible with

---

[13] T. E. Talpey, Reference 13b, Chapter 4.

respect to shot noise so that $\overline{v_k^2}$ may be eliminated. Below 15 Mc the induced grid noise is usually negligible.

(a) *Shot Noise in a Grid-Controlled Tube*

To derive an expression for the shot noise in a grid-controlled tube, we consider the control grid and the cathode to comprise an equivalent diode.[14] The results of Section 13.1(d) are applied to this diode to determine the shot noise current. Assuming that the grid does not intercept or alter this current, this will then be the noise current reaching the anode and appearing in the output circuit, neglecting transit-time effects.

The reduced shot noise current for a space-charge limited diode is obtained from Equation (13.1-37) as

$$\overline{i_s^2} = 4k\theta T_e g_a \Delta f \tag{13.2-1}$$

where

$$g_a = \frac{1}{r_a} = \frac{3}{2}\frac{I_{ao}}{V_{geo}} \tag{13.2-2}$$

is the conductance of the equivalent diode consisting of cathode and control grid; V_{geo} is the equivalent voltage which would have to be placed at the plane of the control grid so as to obtain the current I_{ao} in a parallel-plane diode of the same electrode spacing. This voltage is obtained from Equation (5.2-13) as

$$V_{geo} = \sigma\left(V_{go} + \frac{V_{ao}}{\mu}\right) \tag{13.2-3}$$

where

$$\sigma = \left[1 + \frac{1}{\mu}\left(\frac{d_{ca}}{d_{cg}}\right)^{4/3}\right]^{-1} \tag{13.2-4}$$

We are assuming that the conditions leading up to Equations (5.2-13) and (13.1-37) are fulfilled; that is, we assume that the spacing from the potential minimum to the grid is much greater than the spacing from the potential minimum to the cathode. The transconductance g_m is obtained by differentiating Equation (5.2-13) as

$$g_m = \frac{\partial I_{ao}}{\partial V_{go}} = \frac{3}{2}\sigma\frac{I_{ao}}{V_{geo}} \tag{13.2-5}$$

where use has been made of the definitions given by Equations (13.2-3)

---

[14]Reference 13.8.

and (13.2-4). Combining Equations (13.2-2) and (13.2-5), with V_{ao} given by V_{geo}, we obtain

$$g_m = \sigma g_a \tag{13.2-6}$$

so that the noise current is given by

$$\overline{i_s^2} = \frac{4k\theta T_c g_m \Delta f}{\sigma} \tag{13.2-7}$$

using Equation (13.2-1).

Since σ generally ranges between 0.5 and 1 and θ is approximately 2/3, Equation (13.2-7) states that the shot noise in a grid-controlled tube is equal to the thermal noise generated by a resistor whose temperature is 2/3 to 4/3 the cathode temperature, the conductance of the resistor being equal to the transconductance of the tube.

Noise calculations are often facilitated by representing the shot noise by a passive resistor at room temperature in series with the grid lead of value R_{eq} and an equivalent tube with zero shot noise. The thermal noise current appearing in the plate lead due to this resistor is given by

$$\overline{i^2} = g_m{}^2 4kTR_{eq}\Delta f \tag{13.2-8}$$

Equating Equations (13.2-7) and (13.2-8) we obtain

$$R_{eq} = \frac{\theta T_c}{\sigma T g_m} \tag{13.2-9}$$

which, for a typical tube using an oxide-coated cathode, becomes approximately

$$R_{eq} = \frac{2.5}{g_m} \tag{13.2-10}$$

Measured values[15] of R_{eq} are given in Table 13.2-1 for several common receiving tubes. All of these tubes are triode connected; that is, the plate is connected to the screen grid and suppressor grid in the case of tetrodes and pentodes.

Finally, one may express the reduced shot noise for a grid-controlled tube in terms of a space-charge reduction factor, that is,

$$\overline{i_s^2} = \Gamma^2 \cdot 2eI_{ao}\Delta f \tag{13.2-11}$$

where expressions for Γ^2 may be obtained from Equations (13.2-7) through (13.2-10)

---

[15]T. E. Talpey, Reference 13b, p. 175.

All of the above expressions may be used for the shot noise in a tetrode or pentode provided we define σ properly. This is accomplished by replacing V_{ao} and d_{co} in Equations (13.2-3) and (13.2-4) by the screen-grid voltage and the screen-grid-to-cathode spacing, respectively. I_{ao} in Equation (13.2-11) is the anode current, which might be considerably less than the cathode current if the screen-grid interception is high.[16]

TABLE 13.2-1. MEASURED NOISE QUANTITIES AT 30 Mc*

Tube (Triode Connected)	*Transconductance g_m Micromhos*	*Shot Noise, Equivalent Resistance R_{eq}, Ohms*	*Induced Grid Noise, Equivalent Conductance G_{eq}, Micromhos*
6AG5	6000	480	140
6AK5	5500	460	45
6AU6	6600	420	210
6BC5	5800	590	130
6BC6	7300	410	175
6J6	4400	720	60
396A/2C51	5400	550	40
404A	16000	240	70

*Courtesy M.I.T. Press, Massachusetts Institute of Technology, Cambridge, Mass.

(*b*) *Induced Grid Noise*

At frequencies greater than 15 Mc the noise current induced in the anode circuit of a triode amplifier stage is found to be greater than that predicted by the shot noise theory of the previous section plus the additional thermal noise due to the grid resistance. This additional noise is caused by noise currents which are induced in the impedance of the grid circuit and which, in turn, cause noise voltages to appear between grid and cathode.

Figure 13.2-2 shows qualitatively the current induced in the grid circuit by the passage of a single electron from the cathode to the anode. The total current induced in the grid circuit is the sum of that arising from each of the electrons in transit. Since there are fluctuations in the rate of emission from the cathode, the total current induced in the grid circuit fluctuates so that a noise voltage appears across the impedance of the grid circuit in addition to that arising from thermal noise. This voltage causes the beam to be modulated and consequently increases the fluctuations in the current induced in the anode circuit. The induced grid noise increases as the square of the frequency; and at frequencies greater than 100 Mc, it

[16] *Ibid*, pp. 177–180.

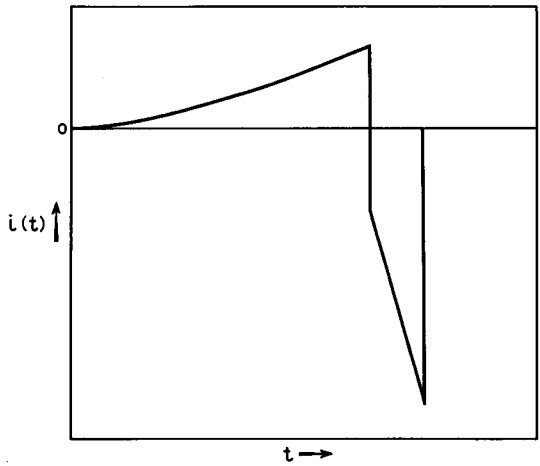

FIG. 13.2-2 Current induced in the grid circuit of a triode due to the passage of a single electron from the cathode to the anode.

is a principal limiting factor in the design of low-noise amplifiers using grid-controlled tubes.

From the physical description of the induced grid noise given above, it is evident that there is a relationship to the input conductance of the grid discussed in Section 7.3(b). The theory of that section may be applied to electrons having shot noise fluctuations with the result that the induced grid noise is given by a noise current generator of value[17]

$$\overline{i_{ig}^2} = 4k\beta T G_{in} \Delta f \tag{13.2-12}$$

where T is equal to room temperature, G_{in} is the input conductance discussed in Section 7.3(b), and

$$\beta = 1.43 \frac{T_c}{T} \tag{13.2-13}$$

equal to approximately 5 for oxide-coated cathodes. The induced grid noise predicted by this equation arises from the shot noise fluctuations in the convection current passing through the grid. Thus, there is a correlation[18] between this noise and the shot noise in the anode current described in part (a) of this section. This correlation must be taken into account in any noise calculations.

---

[17]Reference 13.9.

[18]If the product of two noise currents has a nonzero time average, the currents are said to be correlated.

In addition to the correlated component of induced grid noise described above, there is an uncorrelated component[19] which may be as much as 70 per cent of the total induced grid noise. This uncorrelated component is thought to arise from three major sources;

1. Equation (13.2-12) is derived assuming a uniform transit time for all electrons. In reality, some electrons move closer to the negative grid wires than others, these electrons having thus a longer transit time. The randomness of this transit time introduces an additional induced grid noise.
2. A small percentage (2 to 3 per cent) of electrons elastically reflected from the anode find their way back to the grid, inducing additional noise currents. Since elastic reflections are purely random, and there is no space-charge smoothing of this current of electrons, this contributes significantly to the uncorrelated induced grid noise.
3. Electrons with insufficient emission velocity to pass the potential minimum induce current in the grid circuit if the total transit time is a significant portion of an rf cycle. This "total emission noise" is of course uncorrelated with the current passing the potential minimum.

Just as the shot noise may be replaced by a resistor R_{eq} in the grid circuit, so also may we represent the total induced grid noise by an equivalent shunt conductance G_{eq} in the grid circuit. This conductance is placed from the grid to the cathode; thus an rf short from grid to cathode eliminates induced grid noise. Since R_{eq} is in series with the grid lead, a similar rf short does not eliminate the shot noise contribution. Measured values[20] of G_{eq} are given in Table 13.2-1 for several common tubes.

(c) *Partition Noise*

Since the screen grid of a tetrode or pentode is at a positive potential, it collects a portion of the beam current, and since the electrons have random components of transverse velocity, the rate of collection of electrons by the screen grid fluctuates in time. As a result, the current passing on to the anode also fluctuates, these fluctuations being in addition to the reduced shot noise already present in the beam. Noise of this type, introduced by the random division of current between two or more positive electrodes, is known as partition noise.

As a result of partition noise, the noise generated by tetrodes and pentodes is often three to five times as great as that generated by the same tube connected as a triode.

Since the normal and transverse velocity components of electrons are uncorrelated, the shot noise and partition noise are also uncorrelated.

[19] T. E. Talpey, Reference 13b, pp. 166–176.
[20] *Ibid.*

The following expressions for the partition noise sources indicated in Figure 13.2-1 may be derived:[21]

$$\overline{i_p^2} = (1 - \Gamma^2) \cdot 2e\frac{I_{sgo}I_{ao}}{I_{ko}}\Delta f \tag{13.2-14}$$

$$\overline{i_{sg}^2} = \Gamma^2 \cdot 2eI_{sgo}\Delta f \tag{13.2-15}$$

where I_{ao}, I_{ko}, and I_{sgo} are the dc anode, cathode, and screen-grid currents, respectively, and Γ^2 is the space-charge reduction factor defined by Equation (13.2-11).

If we assume that the noise source $\overline{i_{sg}^2}$ is effectively bypassed by the screen-grid capacitor, the total anode noise is given by the summation of Equations (13.2-11) (reduced shot noise) and (13.2-14) (partition noise), with the result

$$\overline{i_s^2} + \overline{i_p^2} = \left[\frac{\Gamma^2 I_{ao} + I_{sgo}}{I_{ko}}\right]2eI_{ao}\Delta f \tag{13.2-16}$$

An upper limit to the anode noise is obtained by setting Γ^2 equal to unity in the above equation, corresponding to no space-charge smoothing of the shot noise. One obtains

$$\overline{i_s^2} + \overline{i_p^2} = 2eI_{ao}\Delta f \tag{13.2-17}$$

the expression for full shot noise. Thus, despite partition noise effects, the total anode noise can never be greater than that corresponding to full shot noise in the anode current. Physically, this corresponds to the fact that without space-charge smoothing the electron arrival times are completely random, and random interception of some of these electrons cannot increase the randomness of a process that is already completely random.

One may define a noise equivalent grid resistor R_{eq} by Equation (13.2-8) as for the triode. Its value may be obtained by equating Equations (13.2-8) and (13.2-16). This resistor replaces all the anode noise of the tube, that is, shot noise plus partition noise. Hence, values of R_{eq} for tetrodes and pentodes are three to five times as large as the values given in Table 13.2-1.

(*d*) *Flicker Noise and Other Miscellaneous Noise Sources*

Flicker effect or cathode-coating noise becomes important at low frequencies and may determine the ultimate sensitivity of an audio amplifier. Its magnitude is inversely proportional to frequency, and it is usually negligible at frequencies above 100 kc.

Present theory[22] indicates that flicker effect is due to fluctuations of the

---

[21]T. E. Talpey, Reference 13b, pp. 177–180.
[22]A. van der Ziel, Reference 13b, Chapter 2.

voltage drop across a thin surface layer (depletion layer) on the oxide coating of the cathode. Because of the porous nature of the oxide coating, it is proposed that the fluctuating surface layer voltage modulates the current coming from the pores. For further discussion of the theory, the reader is referred to the reference cited.

Another possible source of noise in grid-controlled tubes is secondary-emission noise. Secondary electrons emitted from the anode which go to other electrodes result in fluctuations of the anode current. This noise is minimized by choosing proper dc electrode voltages such that the secondary electrons from the anode are returned to the anode.

Other sources of tube noise include noise due to ionized gas in the tube, poor electrode contacts, leakage currents along the surfaces of insulators, primary emission from the control grid, charges building up on the glass envelope, microphonics due to mechanical vibrations of electrodes, and hum caused by heater current induction. All of these sources of noise can be reduced to a negligible level with proper design and operating conditions.

(e) *Amplifier Stage Noise Figure Calculation*

In this part we shall derive an expression for the spot noise figure of an amplifier stage with an equivalent circuit similar to that given in Figure 13.2-3. This may be assumed to be the equivalent circuit of either a triode, tetrode, or pentode, where for simplicity we have assumed that the anode-to-grid capacitance has been neutralized and that input and output capacitances have been tuned out by shunt inductances. Thus, all impedances are purely real, for simplicity. This is done so that we can concentrate our attention on the noise properties of the amplifier without worrying about the complex circuit analysis required with reactances present.

The expression for the spot noise figure is obtained from Equation (13-4) as

$$F = 1 + \frac{N_a}{\mathcal{G}_o k T_o \Delta f} \tag{13.2-18}$$

where N_a is the available noise power of the amplifier in the bandwidth Δf, and the other symbols are as defined in connection with Equation (13-4).

The available power gain $\mathcal{G}_o$ is defined as the ratio of the powers available at the output and input of the amplifier. The available power at the input is the power available from the source, given by

$$P_{a1} = \frac{|I_s|^2}{4G_s} \tag{13.2-19}$$

The available power at the output is given by

$$P_{a2} = \frac{g_m^2 |I_s|^2}{4(G_s + G_g + G_{in})^2 G_e} \tag{13.2-20}$$

where

$$G_e = \frac{1}{r_a} + \frac{1}{R_L} \tag{13.2-21}$$

The available power gain is thus

$$\mathcal{G}_o = \frac{P_{a2}}{P_{a1}} = \frac{g_m^2 G_s}{(G_s + G_g + G_{in})^2 G_e} \tag{13.2-22}$$

Next we calculate the available output noise due to noise sources within the amplifier. Assuming that the frequency is high, the noise sources are

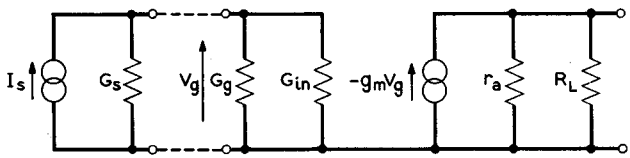

FIG. 13.2-3 Simplified equivalent circuit of a triode, tetrode, or pentode amplifier stage. The parameters are:

I_s Current generator representing the source
G_s Equivalent source conductance
G_g Grid conductance
G_{in} Grid input conductance due to beam loading (Section 7.3(b))
r_a Dynamic anode resistance
R_L Plate circuit load resistance

induced grid noise, anode noise due to shot noise and partition noise, and thermal noise arising from the grid conductance G_g and the anode resistance $R_L = 1/G_L$. All of these noise sources are uncorrelated, except for the correlation between induced grid noise and shot noise discussed in Section (b). For simplicity we shall take the correlation between these noise sources to be zero. Expressions including this correlation and the effects of circuit reactance are derived elsewhere.[23]

The amplifier noise current produced in the grid circuit is given by

$$\overline{i_1^2} = 4kTG_g\Delta f + \overline{i_{ig}^2} = 4kT(G_g + G_{eq})\Delta f \tag{13.2-23}$$

using the definition of G_{eq} given in Section (b). The noise voltage appearing in the grid circuit is given by[24]

$$\overline{v_1^2} = \frac{\overline{i_1^2}}{(G_s + G_g + G_{in})^2} = \frac{4kT(G_g + G_{eq})\Delta f}{(G_s + G_g + G_{in})^2} \tag{13.2-24}$$

[23]T. E. Talpey, Reference 13b, pp. 188–204.

[24]Note that the effect of induced currents in the grid circuit is taken into account by two separate factors. G_{in} expresses the loading at the signal frequency and is noiseless. G_{eq} gives the noise contribution but does not affect the loading at the signal frequency.

Note that, although G_s and G_{in} are not amplifier noise sources, they do influence the noise voltage developed. The noise current appearing in the anode circuit due to this noise voltage is given by

$$\overline{i_2^2} = g_m^2 \overline{v_1^2} = \frac{4kTg_m^2(G_g + G_{eq})\Delta f}{(G_s + G_g + G_{in})^2} \tag{13.2-25}$$

The noise current appearing in the anode circuit due to the shot noise, partition noise, and plate load resistor is given by

$$\overline{i_3^2} = \overline{i_s^2} + \overline{i_p^2} + 4kTG_L\Delta f = 4kT(g_m^2 R_{eq} + G_L)\Delta f \tag{13.2-26}$$

where R_{eq} was defined in Section (c).

The available output noise is given by

$$N_a = \frac{\overline{i_2^2} + \overline{i_3^2}}{4G_s} = kT\Delta f\left[\frac{g_m^2(G_g + G_{eq})}{G_s(G_s + G_g + G_{in})^2} + \frac{g_m^2 R_{eq} + G_L}{G_s}\right] \tag{13.2-27}$$

Substituting this equation and Equation (13.2-22) into (13.2-18), we obtain the desired expression for the spot noise figure:

$$F = 1 + \frac{G_g}{G_s} + \frac{G_{eq}}{G_s} + \left[R_{eq} + \frac{G_L}{g_m^2}\right]\frac{(G_s + G_g + G_{in})^2}{G_s} \tag{13.2-28}$$

where it has been assumed that room temperature T is equal to the standard noise temperature T_o of 290°K.

Let us calculate the noise figure of a typical high frequency (30 Mc) triode amplifier stage using this formula. Assume the following parameters:

$$G_s = 300 \text{ micromhos}$$
$$G_g = 35 \text{ micromhos}$$
$$G_{eq} = 50 \text{ micromhos}$$
$$G_{in} = 17 \text{ micromhos}$$
$$G_L = 10 \text{ micromhos}$$
$$R_{eq} = 450 \text{ ohms}$$
$$g_m = 5000 \text{ micromhos}$$

With these parameters substituted into Equation (13.2-28), one obtains

$$F = 1 + 0.117 + 0.164 + 0.186 + 0.0002 = 1.47$$

which is equal to 1.67 db. The factors in this expression are arranged in the same order as in Equation (13.2-28) so as to illustrate the relative contribution of each noise source. Immediately evident is the fact that thermal noise due to resistance in the anode circuit is negligible compared with the other quantities, and thus in general this term can be neglected.

The expression for the noise figure which applies when reactances are present is[25]

$$F = 1 + \frac{G_g}{G_s} + \frac{G_{eq}}{G_s} + \frac{1}{G_s}\left[R_{eq} + \frac{G_L}{g_m^2}\right][(G_s + G_g + G_{in})^2 + \omega^2(C_s + C_c + C_1)^2] \quad (13.2\text{-}29)$$

where C_s is the source capacitance, C_c is the grid-circuit capacitance, and C_1 is the "cold" input tube capacitance (i.e., the input capacitance without beam loading). Here negative susceptances are represented by equivalent negative values of C_s or C_c. Examining this equation, we see that minimum noise figure is obtained when the net inductance of the source and grid-circuit resonates with the "cold" input tube capacitance. This does not necessarily correspond to the frequency of maximum gain, due to the detuning effect of the susceptance due to beam loading.

13.3 Noise in Microwave Tubes

Either traveling-wave, backward-wave, or klystron amplifiers can serve as low noise amplifiers at microwave frequencies. The same basic theoretical considerations of low noise design apply to each of these devices. However, most low-noise research work has been done on the traveling-wave amplifier, with the result that this particular device has been produced with the lowest noise figures. Thus, we shall concentrate our study on the traveling-wave amplifier.

There are many sources of noise in the traveling-wave amplifier. Thermal noise arises from the attenuation of the helix. Random emission current (shot noise) and random emission velocities result in initial noise current and noise velocity on the electron beam as it enters the helix, both of which are amplified and appear as output noise. Partition noise may arise from interception on the electrodes of the electron gun or on the helix itself. Secondary electrons can also contribute noise. Most of these noise sources can be minimized in low-noise tubes by obvious means. Copper plating of the helix is used to minimize attenuation. Proper focusing of the beam minimizes beam interception, and the collector in low-noise tubes is usually operated at a positive potential with respect to the helix to recapture secondary electrons emitted from the collector. Minimizing the noise due to the emission fluctuations is much more subtle and will constitute the greater part of our discussion.

---

[25]T. E. Talpey, Reference 13b, p. 200.

(a) *Velocity and Current Fluctuations in the Electron Beam*

In order to study the effects of the velocity and current fluctuations in the electron beam, we shall make use of the space-charge wave theory of Section 9.3 and the Llewellyn-Peterson equations of Section 7.2. Both of these theories concern the propagation of small, sinusoidal perturbations on an electron beam. How then can we apply these theories to noise perturbations which are small but certainly not sinusoidal? Suppose we measure and plot as a function of time the instantaneous current and velocity fluctuations of an electron beam over some finite time interval. These functions may be analyzed by means of the Fourier integral to obtain an equivalent sinusoidal current and velocity for a frequency interval Δf. Thus, the propagation of noise perturbations may be determined from the propagation of the equivalent sinusoidal quantities. These equivalent sinusoidal quantities may be related to the corresponding noise fluctuations by equating the integral of the noise power density spectrum over the frequency interval Δf to the power of the equivalent sinusoidal signal.

Let us study the propagation of such waves in a space-charge limited diode connected at the anode to a drift region. We shall first confine our study of the diode to the region from the potential minimum to the anode. The diode may be analyzed using the Llewellyn-Peterson equations of Section 7.2, where plane A is taken at the potential minimum and plane B at an arbitrary plane up to and including the anode. Assuming that the diode is open-circuited at the frequency of interest, the total rf beam current density J_T is equal to zero in Equations (7.2-1). The entrance conditions at plane A are assumed to be a convection current equivalent to full shot noise, Equation (13.1-13), and an ac velocity given by Equation (13.1-24). The initial current and velocity fluctuations are assumed to be uncorrelated, so that the equivalent sinusoidal quantities have no fixed phase relationship. Thus, we consider each initial quantity separately, independent of the other.

We may write our results directly in terms of the noise fluctuations. Since the mean-square values of the noise fluctuations are proportional to the square of the magnitudes of the equivalent sinusoidal quantities, we have from Equations (7.2-1) and (13.1-13) the following results for the shot noise:

$$\overline{i_1^2} = |E^*|^2 \overline{i_A^2} = |E^*|^2 2eI_o\Delta f$$

$$\overline{u_1^2} = \frac{1}{S^2}|H^*|^2 \overline{i_A^2} = \frac{1}{S^2}|H^*|^2 2eI_o\Delta f \tag{13.3-1}$$

where the subscript 1 is used to denote the contribution of shot noise current fluctuations to the convection current and velocity at an arbitrary plane.

S is the beam area. Similarly, we have for the uncorrelated initial velocity fluctuations, from Equations (7.2-1) and (13.1-24):

$$\overline{i_2^2} = S^2 |F^*|^2 \overline{u_A^2} = S^2 |F^*|^2 \frac{ekT_c \Delta f}{mI_o}(4 - \pi)$$

$$\overline{u_2^2} = |I^*|^2 \overline{u_A^2} = |I^*|^2 \frac{ekT_c \Delta f}{mI_o}(4 - \pi) \qquad (13.3\text{-}2)$$

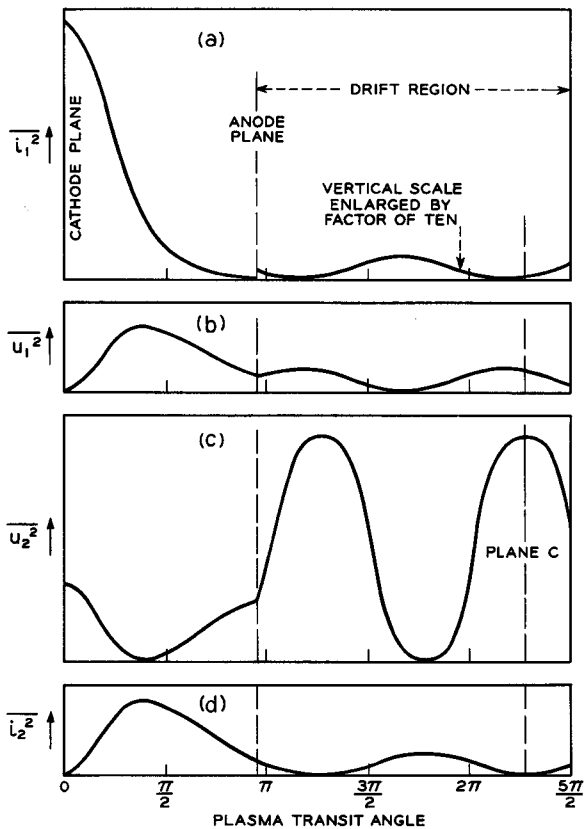

FIG. 13.3-1 Noise standing waves in a particular space-charge limited diode and the drift region following the anode. The noise due to shot noise and initial velocity fluctuations are assumed to be uncorrelated. Distance is measured in terms of plasma transit angle from the potential minimum. (a) Convection current fluctuations $\overline{i_1^2}$ due to shot noise. (b) Velocity fluctuations $\overline{u_1^2}$ due to shot noise. (c) Velocity fluctuations $\overline{u_2^2}$ due to initial velocity fluctuations at the potential minimum. (d) Convection current fluctuations $\overline{i_2^2}$ due to initial velocity fluctuations.

where the subscript 2 is used to designate the contribution of intitial velocity fluctuations to the convection current and velocity at an arbitrary plane. The coefficients E^*, H^*, F^*, and I^* are functions of the location of this plane.

The results of this analysis are shown in Figure 13.3-1, calculated for a particular diode. In Figure 13.3-1(a) is shown the mean-square value of the convection current fluctuations $\overline{i_1^2}$ resulting from the shot noise current at the potential minimum. In Figure 13.3-1(b) is shown the mean-square value of the associated rf velocity fluctuation $\overline{u_1^2}$. Note that the abscissa is the plasma transit angle measured from the potential minimum. The location of the anode has been arbitrarily chosen. In parts (c) and (d) of the figure are shown the corresponding quantities $\overline{u_2^2}$ and $\overline{i_2^2}$ due to the initial velocity fluctuations at the potential minimum.

At the anode plane, the beam enters a drift region at anode potential, and the rf quantities vary in the axial direction with an envelope determined by the plasma wavelength as in Figure 9.3-4. The maxima of $\overline{i_1^2}$ and $\overline{u_1^2}$ in the drift region are separated by a half-plasma wavelength. It should be emphasized that these are standing wave patterns, stationary in space. The phase and amplitude of these standing waves are obtained using Equations (9.3-31) and (9.3-33) by matching boundary conditions at the anode plane. These boundary conditions are that the rf convection current and velocity must both be continuous at the anode plane.

We note from the figure that it is the initial velocity fluctuations rather than the initial shot noise which contributes the major part of the noise of the drifting beam. If we assume a space-charge smoothing factor Γ^2 at the potential minimum, the contribution of the shot noise becomes even smaller in the drifting beam. Thus, the noise produced by using this beam unmodified in a traveling-wave tube results almost entirely from the initial velocity fluctuations.

Since the initial velocity fluctuations contribute so greatly to the noise in the drifting beam, let us study a scheme which has been proposed for reducing this source of noise.[26] Assume that the anode voltage of the diode V_{ao} is small compared with the desired helix voltage. Suppose that the beam is suddenly accelerated to the helix voltage V_o at plane C, shown in Figure 13.3-1. This plane is chosen at the position where the velocity $\overline{u_2^2}$ is a maximum and $\overline{i_2^2}$ is zero. If u_{o-} and Δu_{2-} are the dc velocity and instantaneous velocity fluctuation just before the *velocity jump*, and u_{o+} and Δu_{2+} are the corresponding quantities just after the velocity jump, we have from conservation of energy:

$$(u_{o+} + \Delta u_{2+})^2 - (u_{o-} + \Delta u_{2-})^2 = \frac{2e}{m}(V_o - V_{ao}) \qquad (13.3\text{-}3)$$

[26]Reference 13.10.

where V_{ao} is the diode anode voltage. Expanding the left-hand side and neglecting the terms $(\Delta u_{2+})^2$ and $(\Delta u_{2-})^2$, we obtain

$$2u_{o+}\Delta u_{2+} - 2u_{o-}\Delta u_{2-} = 0$$

or

$$\frac{\Delta u_{2+}}{\Delta u_{2-}} = \frac{u_{o-}}{u_{o+}} = \sqrt{\frac{V_{ao}}{V_o}} \tag{13.3-4}$$

Thus, the bigger the velocity jump, the larger is the reduction of the rf velocity fluctuation.

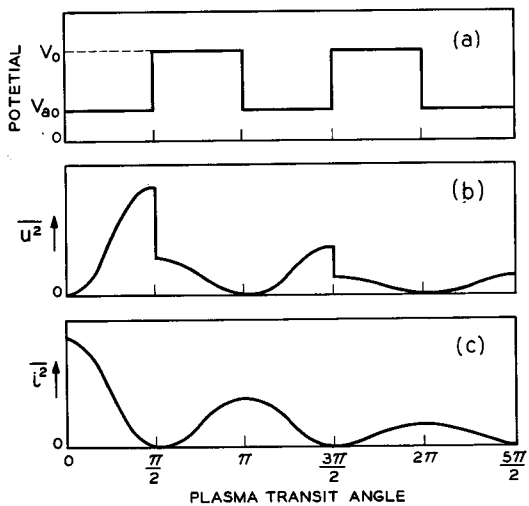

FIG. 13.3-2 Noise reduction resulting from successive velocity jumps. (a) Potential profile along the beam. (b) Velocity fluctuations. (c) Convection current fluctuations.

We may carry the above noise reduction scheme even further. Suppose that at another plane located a quarter-plasma wavelength beyond plane C we suddenly decelerate the beam again. Since the rf velocity is zero at this plane, the principle behind Equation (13.3-4) does not apply and the noise properties of the beam are essentially unchanged. However, now we may introduce another velocity jump a quarter-plasma wavelength farther on and achieve a further noise reduction. Thus, if this process of acceleration-deceleration is repeated N times, the final noise velocity fluctuation $\overline{u_{2(N)}^2}$ is in principle related to the initial fluctuation $\overline{u_2^2}$ by

$$\frac{\overline{u_{2(N)}^2}}{\overline{u_2^2}} = \left(\frac{V_{ao}}{V_o}\right)^N \tag{13.3-5}$$

Since the rf convection current is proportional to the rf velocity from the theory of space-charge waves, the corresponding convection current fluctuations are reduced by the same factor. Thus, one may reduce the noise due to the velocity fluctuations to any desired level merely by choosing enough velocity jump cycles. This process is illustrated in Figure 13.3-2.

Does all of the above discussion mean that we can actually produce a noiseless beam? To answer this question, we must examine the waves due to the shot noise, $\overline{i_1^2}$ and $\overline{u_1^2}$. As drawn in Figure 13.3-1 these waves do not reach their maxima and minima at exactly the same planes as those waves due to the initial velocity fluctuations, $\overline{i_2^2}$ and $\overline{u_2^2}$.[27] Thus, although the noise due to the initial velocity fluctuations can in principle be reduced

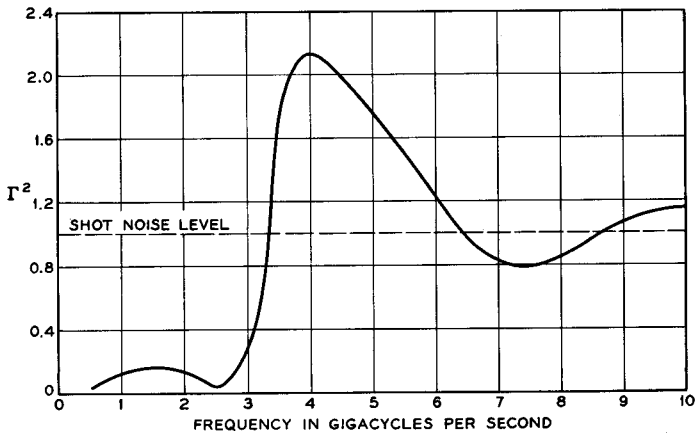

FIG. 13.3-3 Space-charge smoothing factor Γ^2 for the shot noise at the potential minimum as calculated for a typical space-charge limited diode at microwave frequencies. A pronounced dip is obtained at 2500 Mc; this particular diode has a plasma frequency of 3784 Mc at the potential minimum (Reference 13.11). (Courtesy of *J. Appl. Phys.*)

without limit by the velocity jump process, the noise waves due to shot noise cannot be correspondingly reduced. In fact, the lowest noise figure that one can obtain under the above conditions is approximately 6 db.[28]

The foregoing discussion assumed full-shot noise at the potential minimum. Numerical calculations[29] have demonstrated that a space-charge smoothing factor Γ^2 considerably less than unity may be obtained under

[27]This disparity in the phases of the standing waves can be shown to be a general principal. See Reference 13b, Chapters 3 and 5.

[28]H. A. Haus, Reference 13b, Chapter 3.

[29]Reference 13.11.

conditions suitable to a traveling-wave tube. The results of such a calculation are shown in Figure 13.3-3 for a particular diode for which the smoothing is optimized at a frequency of 2.5 Gc. The frequency for minimum Γ^2 is a function of the plasma frequency at the potential minimum; in this case the plasma frequency is equal to 3784 Mc. Different values of the plasma frequency would cause the minimum value of Γ^2 to occur at higher or lower frequencies. This calculation was made numerically assuming charge discs emitted at random times and with random velocities from a cathode, including the forces due to space charge. Physically the smoothing process is analogous to that described in Section 13.1(d), except that transit-time effects become important.

For reduced shot noise, uncorrelated with the velocity fluctuations, the minimum noise figure is given by[30]

$$F = 1 + \Gamma\sqrt{4 - \pi}\,\frac{T_c}{T_o} \tag{13.3-6}$$

which approaches 1 (0 db) as Γ approaches zero. T_c is the cathode temperature.

One additional mechanism of noise reduction remains to be considered. So far we have considered the initial current fluctuations and velocity fluctuations at the potential minimum to be uncorrelated. It can be shown in general[31] that the minimum noise figure decreases as the amount of positive correlation increases. We can see intuitively how such correlation permits further reduction of the noise. Correlation implies a definite phase relation between part of the noise from each of the two noise sources (shot noise and initial velocity fluctuations). If this phase is of the correct value, the two noise sources can be made to cancel each other.

Correlation of the proper type may be produced in the low-velocity region of the diode just beyond the potential minimum. In this region, thermal velocities are of the same order of magnitude as the dc velocity, so that the physical interaction is highly nonlinear. Some ultra-low-noise guns are designed especially to extend this low-velocity region using proper electrode voltages so that the nonlinear noise reduction mechanism is enhanced. Theoretical calculations[32] have indicated that such a low-velocity region can result in a noise figure approaching 0 db. Experimental measurements have also been made demonstrating the existence of such correlation in beams produced by ultra-low-noise electron guns.[33]

Let us return to a further consideration of the velocity-jump noise re-

---

[30]R. W. Peter, Reference 13b, p. 232.
[31]H. A. Haus, Reference 13b, Chapter 3.
[32]Reference 13.12, 13.13.
[33]References 13.14, 13.15.

duction scheme illustrated in Figure 13.3-2. The discontinuities in potential produce strong electric lens effects (Section 3.1) which, despite the strong axial magnetic field used in the gun region, produce a conversion of transverse velocity fluctuations into longitudinal velocity fluctuations. Thus, in practice, it is found that this noise reduction scheme does not result in the lowest noise figures. It is found[34] that a gradual increase in voltage, of the

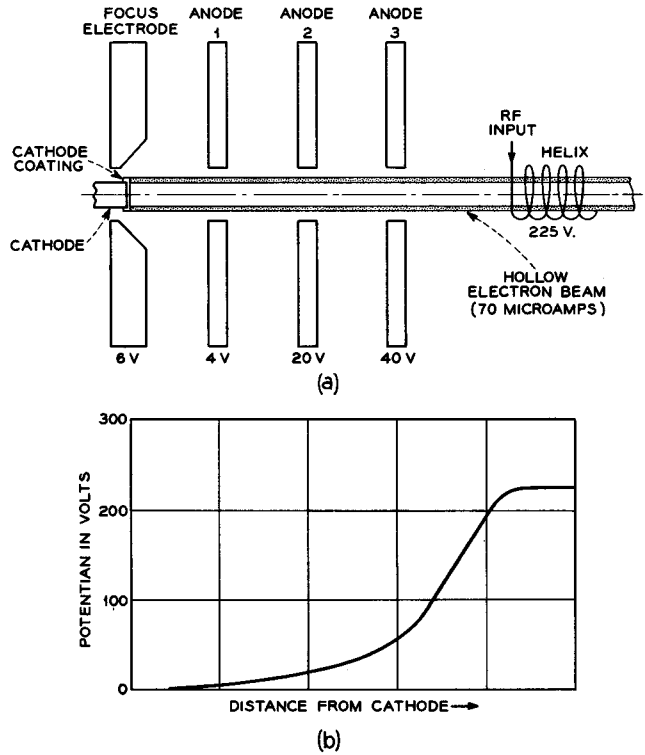

FIG. 13.3-4 Typical ultra-low-noise electron gun. (a) Gun geometry showing voltages applied to the electrodes. (b) Potential variation at the position of the electron beam.

proper variation with distance between the low-velocity diode region and the helix input, can achieve an equivalent noise reduction. In addition, the gradual taper of voltage is effective over a wider frequency band. This voltage variation is analogous to matching two transmission lines of dif-

[34]R. W. Peter, Reference 13b, Chapter 5.

ferent characteristic impedance; the exponential taper is superior electrically to a sudden change of the characteristic impedance.

We may summarize the construction of a typical ultra-low-noise gun in Figure 13.3-4. A strong axial magnetic field confines the electrons to motion in the longitudinal direction; this field is usually stronger than that in the helix-interaction region. Voltages applied to the electrodes produce an extended low-velocity region for the beam near the cathode. This potential distribution results in electron emission which is primarily from the edge of the cathode, producing a hollow beam. Because of this fact some cathodes are made annular, and some are constructed with an additional probe electrode at the cathode center. The oxide coating applied to the end of the cathode also extends a small distance down the cylindrical outer surface of the cathode as shown. It is thought that the intense charge concentration in the beam near the corner of the cathode produces conditions similar to those producing the dip in the space-charge smoothing factor, as predicted in Figure 13.3-3. The extended low-velocity region permits correlation to take place. The gradual increase of voltage to helix potential is carefully shaped so as to result in minimum tube noise figure.

At the time of writing this chapter, the lowest spot noise figure measured on a traveling-wave tube was 1.0 db at a frequency of 2600 Mc.[35] Probably still lower noise figures could be obtained with additional research. One may contrast this value with noise figures which have been measured at microwave frequencies on microwave triodes; values of 16 db or so are common.[36]

Low-noise traveling-wave amplifiers are commonly used as rf amplifiers in sensitive receiver systems. In this application the traveling-wave amplifier provides built-in protection from burnout of the crystal detector following it. As the rf power input to the tube is increased, the rf power output reaches a limiting or saturated value, this value being less than that required to damage the crystal diode.

(*b*) *Description of the Western Electric GA53851 Low-Noise Traveling-Wave Amplifier*

The Western Electric GA53851 is a typical ultra-low-noise traveling-wave amplifier with a noise figure of 4.9 db at frequencies between 5 and 6 Gc. The tube is shown in Figure 13.3-5. Part (a) of the figure shows an outline of the tube together with the corresponding variation of the axial magnetic field used to focus the electron beam. It is to be noted that the magnetic field is peaked in the vicinity of the cathode in order to restrict

[35]Reference 13.16.
[36]Reference 13.17.

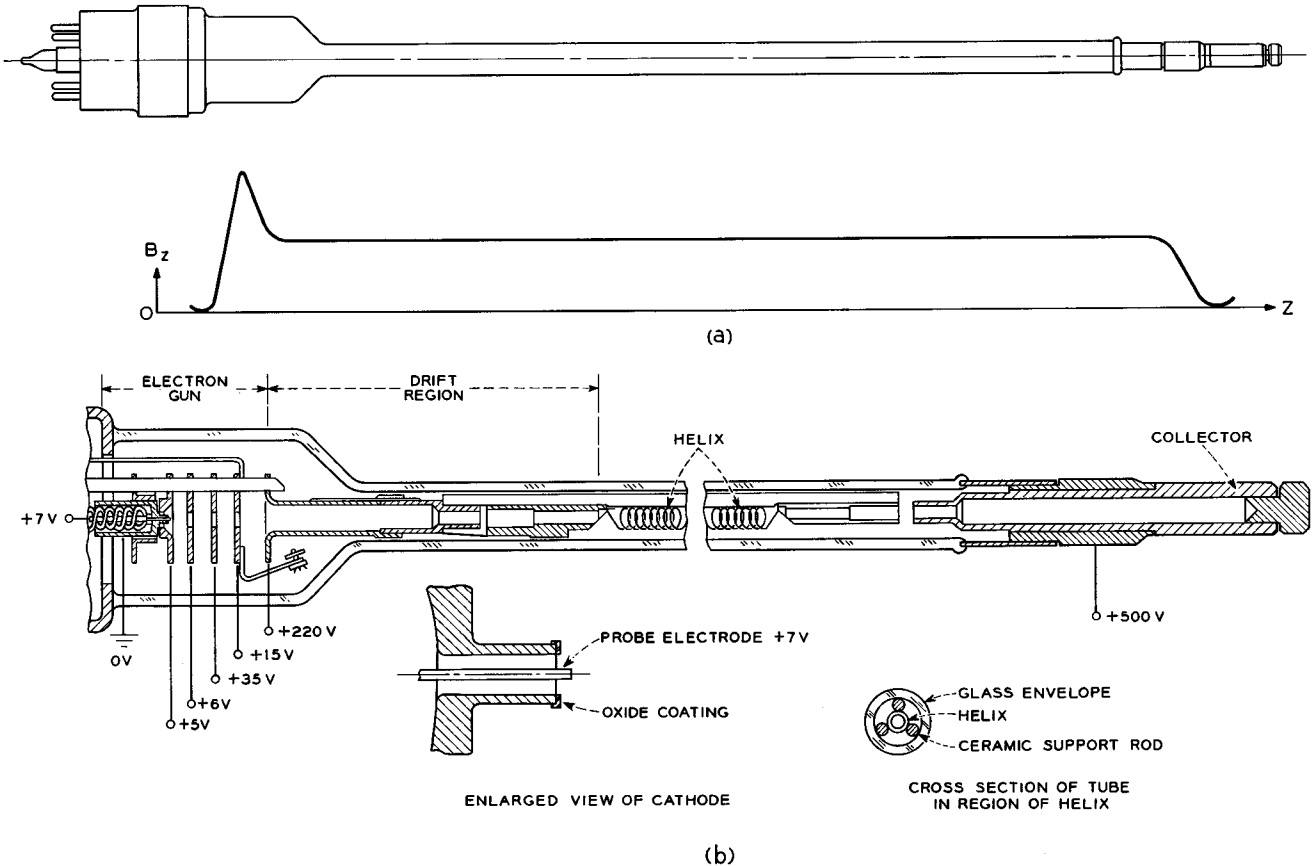

FIG. 13.3-5 Western Electric GA53851. The complete package with magnetic circuit weighs 36 pounds and is 34 cm long. (a) Tube outline showing the corresponding variation of the axial magnetic field. (b) Cross-sectional drawing of the vacuum tube alone showing the values of the applied voltages. The waveguide couplers and magnetic circuit are similar to those of Figure 10.3-7.

transverse motion of the electrons as much as possible in the low velocity region of the electron gun.

The general construction of the tube is shown in Figure 13.3-5(b), exclusive of the waveguide couplers and magnetic circuitry. These additional parts are somewhat similar to those previously shown in Figure 10.3-7. The cathode coating is applied to an annular region at the end of a cylindrical sleeve of nickel. Coaxial with the cathode sleeve is a probe electrode with a positive bias of about 7 volts. The voltages applied to the other electrodes of the electron gun are also shown in the figure. These voltages lead to a potential profile along the electron beam much like that of Figure 13.3-4(b).

The operating characteristics of the tube are presented in Table 13.3-1. The beam current is typically low to minimize the total beam noise at the entrance to the helix. Despite the low beam current, high gain is obtained merely by making the helix long enough. The collector voltage (500 volts) is made much higher than the helix voltage (220 volts) so as to capture within the collector all secondary electrons emitted from the collector. With a lower collector voltage, some secondary electrons from the collector would reach the region of the beam which is inside the helix, and this has been found to degrade the noise figure.

TABLE 13.3-1. WE GA53851 TYPICAL OPERATING CHARACTERISTICS

Frequency, Mc	5000 to 6000
Noise figure, db	4.9
Small-signal gain, db	21
Beam voltage, volts	220
Beam current, ma	60
Saturation power output, mw	0.10

The helix is copper plated molybdenum wire of 0.064 mm diameter. The helix is 13.3 cm long, with a pitch of 0.175 mm and a mean diameter of 1.5 mm. It is glazed to three ceramic rods which support it in the glass envelope of this tube.

The electron gun forms a hollow beam of 0.51 mm inner diameter and 0.74 mm outer diameter. Since the electron trajectories very nearly follow the magnetic field lines, and since the magnetic field decreases from 1250 gauss at the electron gun to 600 gauss in the region of the helix, the beam expands to approximately $1\frac{1}{2}$ times its original diameter by the time it is within the helix.

The complete package of tube, magnet, and waveguide couplers weighs 36 pounds and is 34 cm long.

PROBLEMS

13.1 A temperature-limited diode is connected in series with a resistance R and a battery. The resistance R is at a temperature of 290°K. The dc diode current I_o can be adjusted by varying the cathode temperature. Suppose it is adjusted so that the mean-square noise voltage $\overline{v^2}$ across R, in a frequency band Δf, is just twice the value that existed before the diode was turned on. What is the dc voltage in volts across R with the diode operating under these conditions?

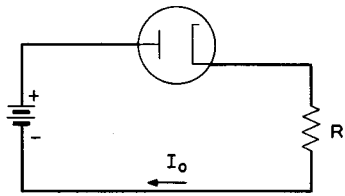

Problem 13.1

13.2 Derive an expression for the mean-square noise voltage appearing at the terminals of a series connection of two resistances R_1 and R_2 at temperatures T_1 and T_2, respectively.

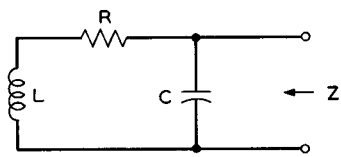

Problem 13.3

13.3 A resistance R, inductance L, and capacitance C are connected together as shown in the figure. The thermal noise generated by the resistance gives rise to voltage fluctuations across the terminals of the capacitance. The input impedance as seen at the terminals of the capacitance is denoted by the symbol Z.

(a) Using one of the noise equivalent circuits of Figure 13.1-2, derive an expression for the mean-square voltage fluctuaiton across the capacitance.

(b) Show that the noise voltage across the capacitance is equal to that of a resistance of value equal to the real part of Z.

13.4 Two identical resistances, each of resistance R, are connected together; both are at the same temperature. Each resistance generates thermal noise which is dissipated in the other resistance. A capacitance C shunts the two resistances; this capacitance represents the stray capacitance inevitably present in any physical circuit.

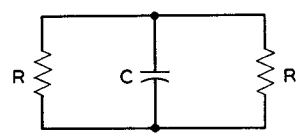

Problem 13.4

(a) Show that the total noise power flowing from one resistance to the other, as integrated over the entire frequency range from zero to infinity, is given by $kT/2RC$.

(b) Show that the average stored energy in the capacitance due to the noise fluctuations is given by $\frac{1}{2}kT$.

13.5 A resistive pad inserted into a transmission line is designed such that its image impedances are equal to the characteristic impedance of the transmission line. The definition of noise figure may be generalized to apply to passive networks,

where the available power gain is less than or equal to unity. Find an expression for the noise figure of a resistive pad inserted into a lossless transmission line which is matched at both ends. What is the noise figure of a pad designed to produce an attenuation of 3 db?

13.6 An amplifier consists of two stages of amplification. The first stage has an available power gain $\mathcal{G}_1$ and a noise figure F_1. The second stage has an available power gain $\mathcal{G}_2$ and a noise figure F_2.

(a) Show that the noise figure of the whole amplifier F_{12} is given by

$$F_{12} = F_1 + \frac{F_2 - 1}{\mathcal{G}_1}$$

(b) If the first stage has a noise figure of 4 db and an available power gain of 20 db, calculate the maximum noise figure of the second stage for an overall amplifier noise figure of 4.5 db.

13.7 Assuming that one has a power meter capable of measuring noise power over the appropriate frequency bandwidth, explain how one could measure the induced grid noise and the reduced shot noise for a triode with the equivalent circuit given in Figure 13.2-3.

13.8 Calculate R_{eq} for a pentode, including the partition noise. The control grid interception is negligible.

$$g_m = 5000 \text{ micromhos}$$

$$I_{ao} = 7 \text{ ma}$$

$$I_{sgo} = 2 \text{ ma}$$

13.9 The noise figure of the amplifier in Figure 13.2-3 is a function of the source conductance G_s. Show that the lowest noise figure is obtained for G_s given by

$$G_s = \sqrt{\frac{G_g + G_{eq}}{R_{eq} + G_L/g_m^2} + (G_g + G_{in})^2}$$

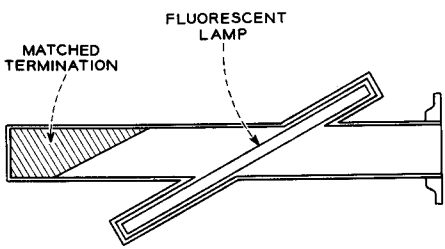

Problem 13.10

13.10 In the fluorescent lamp noise source shown in the figure, the matched termination causes a noise power kTB to flow to a matched load whether the lamp is on or not. When the lamp is on, an *additional* noise power equal to 38 times kTB flows to the load. Suppose that the noise source is connected to the matched input of a traveling-wave amplifier (TWT), and a detector which measures noise power over a band B is connected to the output of the tube. The gain of the traveling-wave amplifier is assumed to be uniform over

the band B. Let

$$X = \frac{\text{noise power output from TWT with lamp on}}{\text{noise power output from TWT with lamp off}}$$

Show that the noise figure of the amplifier is given by

$$F = \frac{38}{X - 1}$$

REFERENCES

Two general references to the material of this chapter are:

13a. A. van der Ziel, *Noise*, Prentice-Hall, Inc., New York, 1954.

13b. L. D. Smullin and H. A. Haus (Eds.), *Noise in Electron Devices*, Technology Press of M.I.T. and John Wiley and Sons, Inc., New York, 1959.

Other references covering specific items are:

13.1 J. M. Pettit and M. M. McWhorter, *Electronic Amplifier Circuits, Theory and Design*, McGraw-Hill Book Co., Inc., New York, pp. 283–285, 1961.

13.2 *IRE Standards on Electron Tubes:* Methods of Testing 1962, Part 9, 1962.

13.3 R. L. Forward and F. Richey, "Effects of External Noise on Radar Performance," *Microwave Journal* **III,** 73–80, December, 1960.

13.4 W. B. Davenport, Jr., and W. L. Root, *An Introduction to the Theory of Random Signals and Noise*, McGraw-Hill Book Co., Inc., New York, 1958.

13.5 H. Nyquist, "Thermal Agitation of Electric Charge in Conductors," *Phys. Rev.* **32,** 110–113, July, 1928.

13.6 J. R. Pierce, "Noise in Resistances and Electron Streams," *Bell System Tech. J.* **27,** 158–174, January, 1948.

13.7 A. J. Rack, "Effect of Space Charge and Transit Time on the Shot Noise in Diodes," *Bell System Tech. J.* **17,** 592–619, October, 1938.

13.8 D. O. North, "Fluctuations in Space-Charge Limited Currents at Moderately High Frequencies," Part II, "Diodes and Negative Grid Triodes," *RCA Rev.* **4,** 441–472, April, 1940; **5,** 106–124, July, 1940.

13.9 D. O. North and W. R. Ferris, "Fluctuations Induced in Vacuum Tube Grids at High Frequencies," *Proc. IRE* **29,** 49–50, February, 1941.

13.10 D. A. Watkins, "Noise Reduction in Beam Type Amplifiers," *Proc. IRE* **40,** 65–70, January, 1952.

13.11 P. K. Tien and J. Moshman, "Monte Carlo Calculation of Noise Near the Potential Minimum of a High-Frequency Diode," *J. Appl. Phys.* **27,** 1067–1078, September, 1956.

13.12 A. E. Siegman, D. A. Watkins, and H. C. Hsieh, "Density-Function Calculations of Noise Propagation on an Accelerated Multi-velocity Electron Beam," *J. Appl. Phys.* **28,** 1138–1148, October, 1957.

13.13 A. W. Shaw, A. E. Siegman, and D. A. Watkins, "Reduction of Electron Beam Noisiness by Means of a Low-Potential Drift Region," *Proc. IRE* **47,** 334–335, February, 1959.

13.14 A. Zacharias and L. D. Smullin, "Noise Reduction in Electron Beams," *Trans. IRE* **ED-7,** 172–173, July, 1960.

13.15 J. M. Hammer, "Measured Values of Noise Spectra, S and Π, of Ultra-Low-Noise Beams," *Proc. IRE* **51**, 390–391, February, 1963.
13.16 J. M. Hammer and E. E. Thomas, "Traveling-Wave-Tube Noise Figures of 1.0 db at S-Band," *Proc. IEEE* **52**, 207, February, 1964.
13.17 M. T. Vlaardingebroek, "Small-Signal Performance and Noise Properties of Microwave Triodes," *Philips Res. Reports* **15**, 124–221, April, 1960.